J. Basic. Appl. Sci. Res., 2(6)6201-6209, 2012

ISSN 2090-4304
Journal of Basic and Applied Scientific Research
www.textroad.com

A Brushless Axial Flux Permanent Magnet Generator with Two Mechanical Powers Inputs for Marine Current Energy Generation

Asghar Safari-Doust[1], Abbas Rezaey[2]

[1]Department of Electrical and Computer Engineering, Semnan University, Semnan, Iran
[2]Department of Electrical Engineering, Islamic Azad University, South Tehran Branch, Tehran, Iran

ABSTRACT

A novel Axial flux Brushless Permanent magnet generator with two mechanical inputs for marine current energy generation is proposed, and a detailed description of its construction is presented. The generator topology consists of two independent counter rotating rotors and a stator, without any brushes and slip rings for excitation system make it make a water proof generator for marine current energy generation. Also, this generator is direct drive with no need gear-box, due to high relative speed between the rotors. Moreover, all components of the generator were modeled and designed using an analytical approach. An optimum design for the generator was obtained using analytical iterative approach. To evaluate the efficiency of the obtained design, flux density simulations using a finite element software package were carried out. The obtained simulation results demonstrated the effectiveness of the proposed generator.
Keywords- Permanent magnet generator, excitation system, Marine curent energy.

NOMENCULTURE

l_m	**Axial length of magnet**
w_m	Width of bar
Y_{R1}	Axial thickens of first rotor back iron
g_1	First Air-gap length
g_2	Second Air-gap length
Y_s	Axial length of stator yoke.
Y_{R2}	Axial length of second rotor yoke
w_s	Slot width
w_t	Teeth width
d_m	Shaft diameter
p	Number of slot per pole
R_i	Inner diameter of rotors and stator
R_o	Outer diameter of rotors and stator
m	Number of phases
d_c	Conductor diameter
N_{cs}	Number of conductors per slot
N_{ph}	Number of series turns per phase per pole

INTRODUCTION

Consumption of fossil fuel as resource of energy cause to global warming and environmental impacts, initiate in green house effects of carbon dioxide gas emission. The renewable energy are the best alternative to address this problem [11]. Marine current energy proposes an enormous a dense layer of energy under seas can be considered as an appropriate alternative energy resource. For instance, it has been estimated that the marine current in Gulf Stream is estimated about 1000 time greater than the Niagara Falls [1, 10]. Advantages of marine current energy over the wind energy are higher power density, minimum aesthetics impacts, and lower noise separation.

In previous research works, some Marine Current Turbine Generators Systems (MCTGSs) for extraction of marine current energy were proposed. Based on installation methods of the MCTGSs, they can be divided to two classes of Fixed MCTGs (FMCTGS) and Buoyant MCTGSs (BMCTGS). The FMCTGSs were installed under the water using a tower. Like the twin-turbine system with horizontal axis turbines mounted on a tower underwater, presented in [2-3].

***Corresponding Author:** Abbas Rezaey, Department of Electrical Engineering, Islamic Azad University, South Tehran Branch, Tehran, Iran

Despite the FMCTGSs, the BMCTGSs are buoyant using a storage filled with air, while were tethered via a reinforced cable to the ground under the water. In [5], a FMCTGS constructed as counter-rotating topology was presented. It employs two independent rotors which are rotating in opposite directions by two turbines.

(a) (b)

Figure 1. (a) Deploymnt of BMCTGS with an air storage. (b) A FMCTGS installed under water.

The key feature of counter rotating topology is minimization of acted torque on the turbine supporting structure which prevents rotation of FMCTGS [4]. Other advantages of contra-rotating topology are lower turbine wake and elimination of gear-box due to high relative speed of rotors [5]. But, one of drawbacks of utilization of second rotor is the need to brushes and slip rings for transferring the generated electrical power by it to stationary terminals of generator. The sea water is conductive, due to salt ions in the water. Thus, the brushes and slip rings cause to a higher maintenance cost in case of water leakage to the generator. Due to deployment of BMCTGS in deep waters and difficultly of their maintenance, the actual trend in marine current energy generation technology is to achieve FMCTGSs with a higher torque to volume ratio and minimum maintenance.

Therefore, it is necessary to design a permanent magnet electrical generator benefits both the counter-rotation and brushless topologies. Thus, in this paper a novel axial flux brushless permanent magnet generator with the needed features is proposed. The differences between the proposed generator and the conventional axial flux permanent magnet generators were summarized in following.

The conventional axial flux permanent magnet generators consist of a rotor and a stator [5]. The rotor is a disk with mounted magnets on it rotating by a prime mover to create a rotating magnetic field in the air-gap. The magnetic field induces electrical voltage in the stator winding. But in the proposed generator in this paper, there are two rotors rotate in opposite directions using two independent prime movers results in rotating magnetic field rotors with relative speed of the rotors between. Consequently, this generator has two mechanical power inputs. Since there are two rotors which are rotating in opposite directions, the brushes and slip rings are required. Thus, for elimination of required brushes and slip rings for the second rotor, we use a stator.

Two mirrored turbines are connected to the first and second rotors shafts'. The complete generator is anchored to the ground under water via a reinforced cable. A storage filled with air provides enough uplifting to support it at a specific height.

The main scientific contributions of this paper are summarized in following. A novel counter rotating topology proposed and modeled. An electrical model proposed using analytical approaches. To reach an optimum design for this type of generator a design procedure is carried out and its efficiency of obtained design is validated.

This paper was organized as follows: in section II, a brief description of all components of the generator is presented. In section III, a design procedure including prediction of the magnetic field magnitude, geometric dimensions to achieve an optimized design, and investigation of the resulted design using a finite element software package is presented. In section IV, to verify the efficiency of the resulted design magnetic flux simulations in the generator cores are carried out. Section V concludes paper.

PROPOSED GENERATOR

The proposed topology consists of two counter rotating independent rotors and a stator. The rotors and the stator are disk shape. Thus, the flux lines in the air-gaps are along the shafts. A simplified side view representation of the generation is shown in Fig. 2. The two rotors are spaced together with first air-gap. The stator is spaced from the second rotor with a second air-gap. As seen there are two independent prime movers, first and second prime movers which are rotating the first and second rotors via the corresponding shafts in opposite directions, while the stator is fixed to the frame.

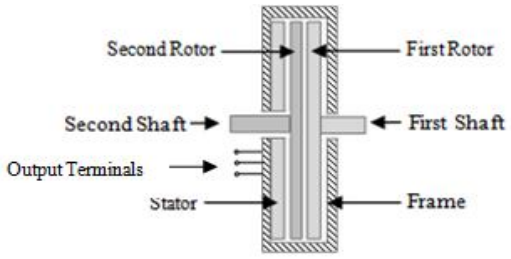

Figure 2. Simplifide side-view representetion of the proposed generator.

A) Fisrt rotor

The first rotor is constructed as a disk shape rotor with mounted magnets on it with arrangement of *N-S-N* as shown in Fig. 3. It will be rotated with the first prime mover. By rotation of the first rotor, a rotating magnetic field will be created in the first air-gap.

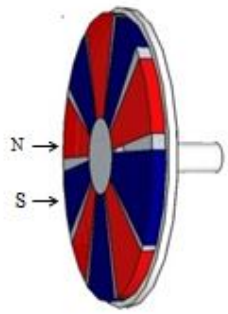

Figure 3. Second disk shape rotor with mounted magnets on it.

B) Second rotor

As shown in Fig. 4(a), the second rotor is a disk which it's both sides are slotted. The right side of this rotor is wound as three phase star connection, and its left side is wound as single phase connection. The three and single phase windings are electrically paralleled using a rectifier, as simply is shown in Fig. 4(b). The second rotor will be rotated by the second independent prime mover in opposite direction of the first rotor.

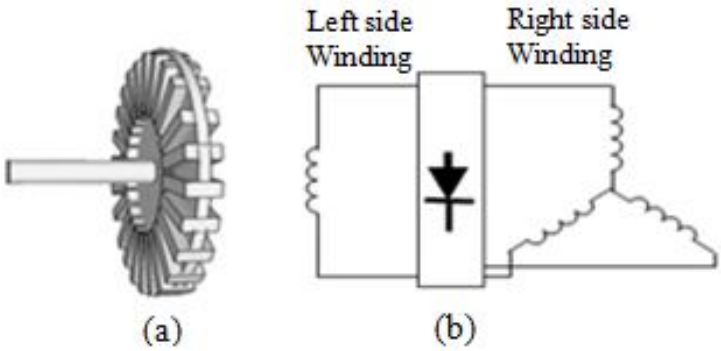

Figure 4. (a) Second rotor. (b) Righ and left sides winding of the second rotor.

C) Stator

The stator is a disk which only right side of it is slotted shown in Fig .5. Stator is the stationary part of generator wound as a three phase connection winding to provide a three phase voltage. The output terminals of winding of this stator are the output terminals of the generator. It should be note that, due to loss in yoke of the stator, the generator loss increase. But, the stator and second rotor operate as a second generator contributes in energy conversion generates more power compensates the loss and increase the generator efficiency.

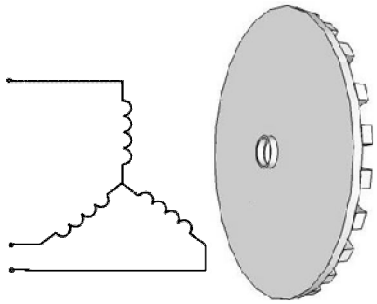

Figure 5. Stator wound as three phase star connection winding.

An assembled representation of generator components is shown in Fig. 6(a). As seen the second rotor is between the first rotor and the stator. A frame axially supports the rotor which is shown in Fig. 6(b). Two mirrored turbine will be connected to the first and second shafts as shown in Fig. 6(c). Thes rotors will be rotated by the turbines in opposite directions.

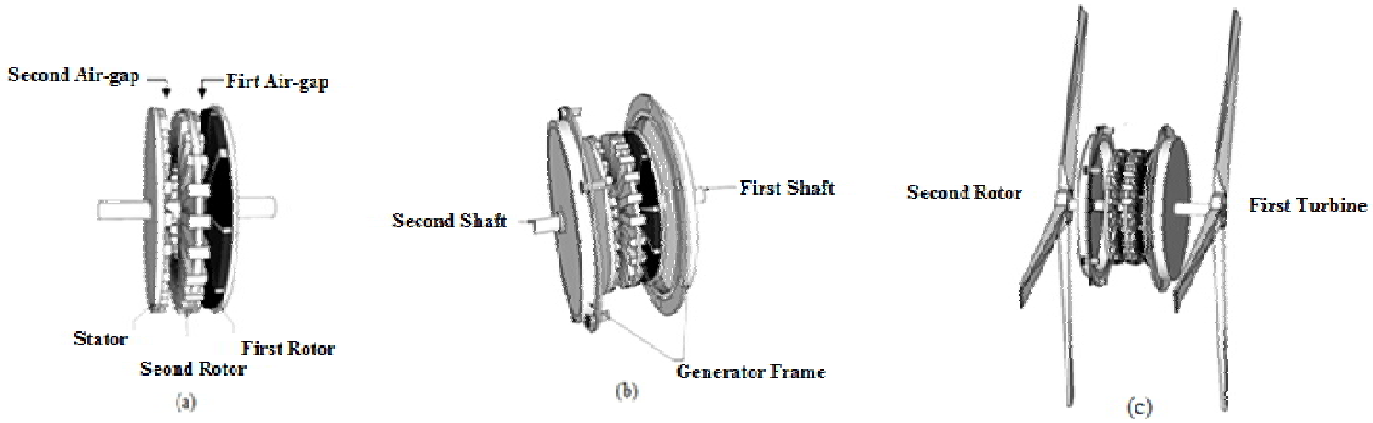

Figure 6. (a) Asemmbely of the generator. (b) Conceptual representation of the generator. (c) two turbines rotating the rotors in opposite directions.

The direct current output voltage of the rectifier feeds the single phase winding of the second rotor. Similarly, since the second rotor is rotating, it creates a rotating magnetic field between the second rotor and the stator, the second air-gap. This rotating magnetic field induces electrical voltage in the three phases winding of the stator, appears in generator output terminals.

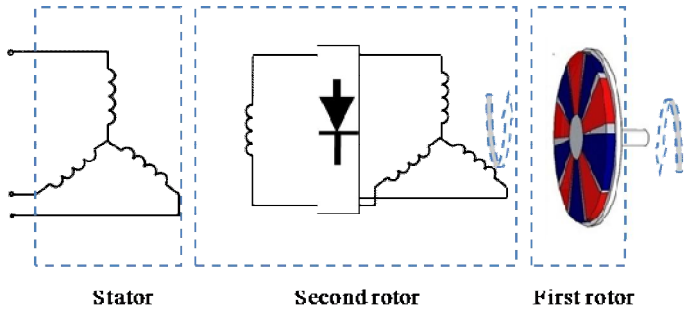

Figure 7. Conceptual representation of the generator.

To present the performance and operation principle of the generator, the rotors and the stator can be considered as linear shapes, as shown in Fig. 8(a). This consideration is being typically used in analysis of electrical machines. As seen in Fig. 8(a), the first and second rotors are moving along together with linear velocities of V_{R1} and V_{R2}, respectively. To convert the angular speeds of ω_{R1}, ω_{R1} to V_{R1}, V_{R2} the following relation are given:

$$v_{R1} = \frac{R_i+R_o}{2}\omega_{R1} \quad (1)$$

$$v_{R2} = \frac{R_i+R_o}{2}\omega_{R2} \quad (2)$$

Where, $R_i$and $R_o$are the inner and outer radius' of the rotors, shown in Fig. 8(b)

Due to the mounted magnets on the first rotor, a magnetic field with relative speed of $V_{R1} + V_{R2}$ and a direction the same direction of the first rotor velocity appears between the first and second rotors, first air gap, as shown in Fig. 8(a). This magnetic field induces a voltage in the primary winding of second rotor, right side of second rotor. The induced voltage can be written as:

$$V = V_m \sin[(\omega_{R1} + \omega_{R1})\, t] \quad (3)$$

$$= V_m \sin[2\frac{v_{R1} + v_{R2}}{R_i + R_i}t]$$

This voltage feeds the left side single phase winding of second rotor. Thus, and a magnetic field with velocity of v_{R2} appears between second rotor and the stator, as can be seen in Fig. 8(a).

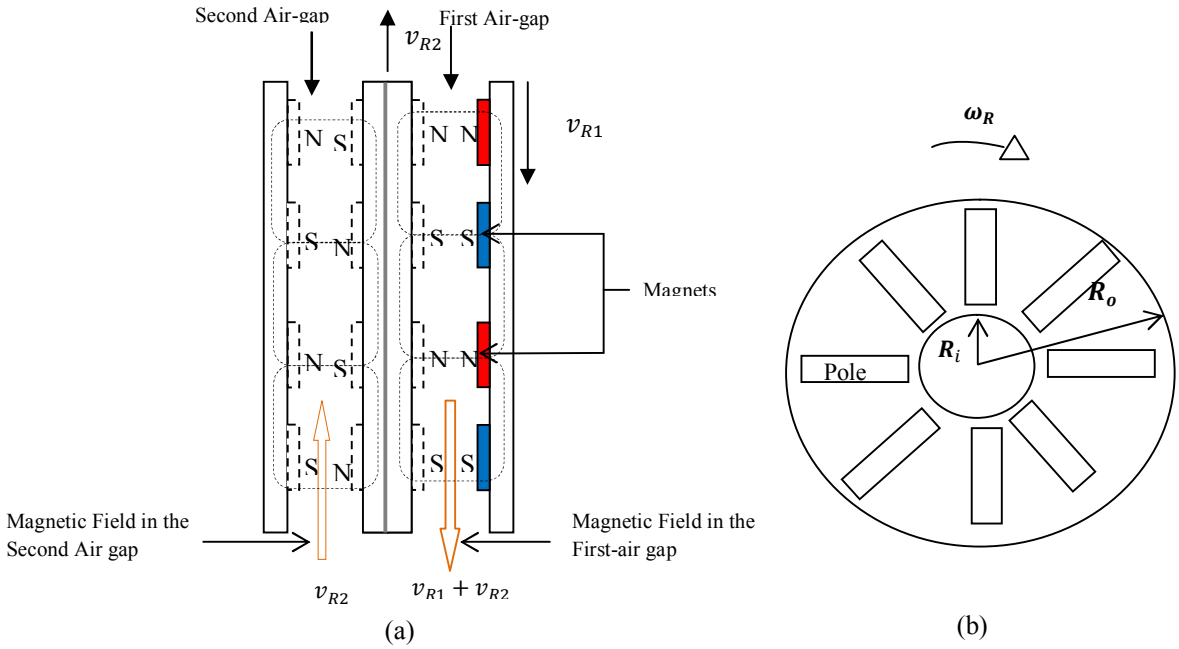

Figure 8. (a) Linear consideration of generator, and the magnetic fields speed in first and second air-gaps. (b) Inner and outer radious of the second rotor and stator.

The induced voltage in stator winding appears in output terminals of generator will be:

$$V_{out} = \frac{V_m}{N} \sin\left(\frac{v_{R1}}{R_i + R_i} t\right) \quad (5)$$

In this topology the second rotor and stator are contributing in energy conversion. This configuration is same as two generators; one of them is feeding the excitation winding of another.

DESIGN PROCESS OF THE GENERATOR

A simple design sketch of the generator with its geometric dimensions is shown in Fig. 9. The dimensions of this design will be determined using one step at a time process presented in following.

A. *Material Selection and Initial data*

The initial data to initiate the design are the magnet, iron, conductor material data, and the air-gaps axial length selected with mechanical constraints.

B. *Selection of User Defined Parameters*

The user defined design parameters are the pole pairs p, and the number of slot per pole per phase, q.

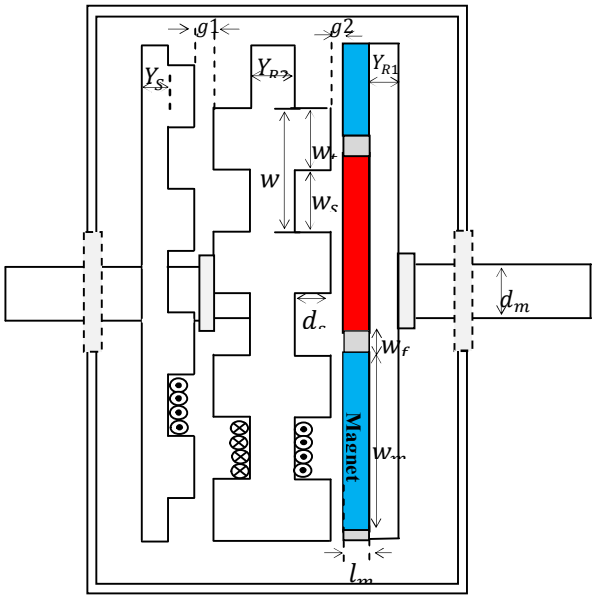

Figure 9. Simple design of the generator with its geometric dimentions

C. *Winding Configuration and Factors*

The configuration of the windings of generator is the same and shown in Fig. 10. These winding are right and left sides of the second rotor windings and the stator winding. The$A$, B and C are the phases and direction of current denoted as signs of the "+" and "−", respectively.

$+A$	$-C$	$-A$	$+C$	$-B$	$+A$	$+B$	$-A$	$-B$

Figure 10. Phases arrangment in the windings.

The winding coefficient is:

$$k_w = k_d k_{sp} k_{sp} \tag{6}$$

Where the k_d, $k_{sp}$and $k_{sp}$are the distributions, skewing and short pith angle factors, respectively. Following [9], these factors are:

$$k_d = \frac{\sin(\frac{p\theta_s}{2})}{p\sin(\frac{\theta_s}{2})} \tag{7}$$

$$k_{sp} = \sin\frac{\theta_s}{2} k_{sp} \tag{8}$$

$$k_{sp} = \frac{\sin\frac{\gamma}{2}}{\frac{\gamma}{2}} \tag{9}$$

D. *Determination of teeth and slot width*

Slot and teeth width were mainly determined by air-gaps flux densities and the ampere loading:

$$w = \frac{R_i\pi}{2pqm} \tag{10}$$

As the flux density in the air-gaps increases, the width of tooth should be increased for avoidance of saturation. The wider tooth cause to a smaller slots and lower space for conductor outcome is a lower output power compared desired rated value. This close relation among the rated power, air-gaps flux densities, the teeth and slot width and the slot depth result in a multipart optimization problem. Thus, we used a simple relation between dimension of teeth and slot to achieve minimize volume in rated power, presented in [10]:

$$w_t = (1 - w_s)w \tag{11}$$

$$\text{Where } 0.5w < w_t < 0.6w$$

But, for simplification of computations, we consider equal slot and teeth width. Thus, the width of slot and teeth will be:

$$w_t = w_s = \frac{\pi R_i}{k_{st}N_s} \cdot \frac{B_g}{B_{sat}} \tag{12}$$

E. *Determination of Magnet and Iron Dimensions*

Since the primary and secondary windings were electrically parallel, created current in right side winding the second rotor winding feeds the left side winding. Consequently, another rotating magnetic field in the second air-gap appears. Since we assumed that the primary and secondly windings are the same in turns and cross sectional areas, the magnetic flux density in second air-gap is equal to calculated armature reaction in first the air-gap. The sinusoidal rotating magnetic flux in second air-gap can be written as:

$$B_{g2} = B_a\cos(p\theta - \omega) \tag{13}$$

Similar approach can be taken for calculation of maximum magnetic field in second the air-gap. The induced voltage in stator winding and the created armature reaction by the stator winding increase the magnetic flux. The armature reaction due the stator is calculated:

$$B_{as} = \frac{\mu_0}{g_2}\frac{3}{2}I\sqrt{2}\frac{N_S}{p} \tag{14}$$

Thus maximum magnitude of the rotating magnetic flux in second air-gap will be:

$$B_{g2max} = B_a + B_{as} \tag{15}$$

$$w_m = \frac{(R_o+R_i)\pi}{2p} \tag{16}$$

F. *Determination of Conductor and Series Turns per Phase*

As the number of series turn per phase, N_{ph}, is founded, the conductor diameter can be calculated as:

$$d_c = 2\sqrt{\frac{k_{sf}A_{slot}}{\pi N_{cs}}} \tag{17}$$

Where, A_{slot} is the area of the slot:

$$A_{slot} = d_{1s}w_s \tag{18}$$

The number of conductor per slot will be:

$$N_{cs} = \frac{N_{ph}}{pq} \tag{19}$$

During operation of the generator the axial length of magnets should be selected so that demagnetization can be slight. The axial length of magnets can be found by multination of first air-gap by premance of used magnet. Based on the [8], the values between 5-20 guarantee this insignificant demagnetization. But, to achieve lower cost, we selected a medium value of 15.

$$l_m = g.PC \tag{20}$$

$$B_{gm} = \frac{B_r}{1+\frac{2g\mu_r}{l_m}} \tag{21}$$

$$w_t = w_s = \frac{\pi R_i}{k_{st}N_s}.\frac{B_g}{B_{sat}} \tag{22}$$

Eq. (27), (22) were iterated until minimum volume is obtained. Then, axial length of magnets can be calculated using eq. (20). After the iteration, not only the resulted values for the slot and teeth widths of rotors guarantee the generator cores is under saturation, but also it ensures minimum volume for the machine.

G. *Determination the Dimension of Rotors and Stator Yokes*

To avoid saturation of the rotors and the stator yoke, thickness of their yokes should be determined by maximum flux densities in the air-gaps:

$$Y_{R1} = Y_{R2} = \frac{\pi R_i \alpha_m}{4k_{st}p}.\frac{B_g}{B_{sat}} \tag{23}$$

$$Y_s = {}^{Y_{R2}}/_{2} \tag{25}$$

Where, α_m pole is pitch coverage of magnet:

$$\alpha_m = \frac{w_m}{w_m+w_f} \tag{26}$$

H. *Determination of the Generator Diameter*

Diameter of machine is closely relates to the number of the series turn per phase N_{ph}. There is a reverse relation between the generator diameter and number of turns per coils. By increasing the series turn turns per phase, the generator diameter decrease. Thus, to determine of a specific diameter N_{ph} should be iterated. For determination of desired generator diameter the number of series turn per phase should be iterated while the diameter meets the desired diameter with minimum volume. Following [8], the losses in a axial flux generator are:

$$P_{gap} = P_{out} + P_{Core} + P_{Copper} \tag{27}$$

$$P_{Copper} = \frac{N_{ph}(2(R_o-R_i)+(r_{co}+r_{ci})\frac{\pi}{2})}{\sigma_{cu}A_{cu}K_p}I^2 \tag{28}$$

$$P_{core} = P_{ir} + P_{mag} \tag{29}$$

$$P_{ir} = P_h + P_e \tag{30}$$

$$= c_h B^n f + c_e B^2 f^2$$

$$P_{mag} = \frac{\sigma}{48} l_m (R_o - R_i)\tau^3 B^2 {w_e}^2 \tag{31}$$

The air-gaps power is axial flux machine can be written as:

$$P_{cov} = 2\pi k_w \sin\left(\frac{\theta_m}{2}\right) {}^{f}\!/_{p} \left(A.B_{g1}\right)(R_o + R_i)^2(R_o - R_i)sin\beta \tag{32}$$

Where, A is current density:

$$A = \frac{6N\sqrt{2}IN_{ph}}{(R_o+R_i)\pi} \tag{33}$$

Since the resulted design with the desired diameters proposes many feasible designs, we use power minimum to weight ratio constraint make it lightweight generator marine current energy generation applications:

$$T = \frac{\pi}{2} k_w B_{g1} A(R_o + R_i)^2(R_o - R_i)sin\beta \tag{34}$$

$$\mathcal{E} = \frac{T}{W} \tag{35}$$

I. *Determination of efficiency*

Following [9], the efficiency of the generator can be expressed as:

$$\eta = \frac{P_{out}}{P_{out}+P_{Core}+P_{Copper}+P_f+P_w} \tag{36}$$

Where, P_w and P_f are the winding and friction losses:

$$P_w = \frac{1}{2} c_f \rho \pi \omega^2 ({R_o}^3 - {R_o}^3) \tag{37}$$

$$P_f = C_o {d_m}^3. \tag{37}$$

OPTIMIZATION PROCEDURE

Flowchart of the optimization design procedure is shown in Fig. 11. Also the input data and resulted design by the iterative approaches are given in Table I

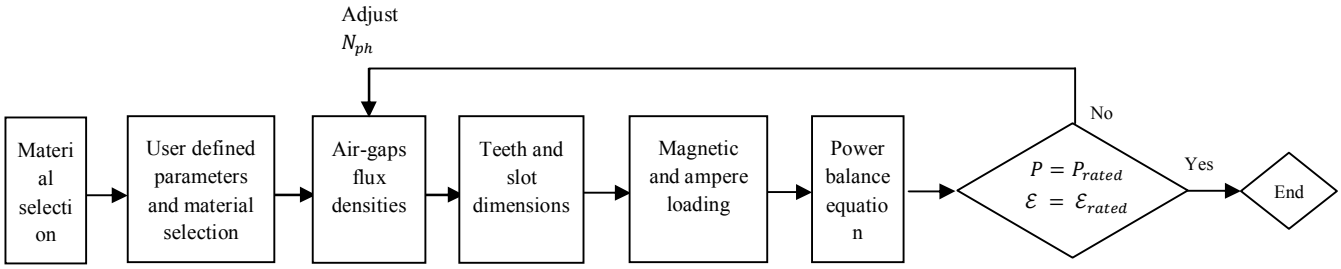

Figure 11. Flowchart of the optimization procedure

TABLE I
INPUT DATA AND DESIGN RESULT

Input Data		Design Result	
Quantity	Value	Quantity	Value
Conductors	AWG 17	Pole pairs numbers, p	4
Air-gaps peak flux density, B_g	0.865 T	Number of slot/ pole/phase	3
Output power, P_{out}	46450 W	Outer dimeter, D_o	230 mm
Ampere loading, A	20312 A/mm^2	Air-gap axial length	0.7 mm
Active power per generator mass	15 kWT /m^3	Axial thikness of bar, l_b	21 mm
Inner diamterer of rotor	90 mm	Apparent power, S	50kVA
Machine axial length	60 mm	No-load phase voltage (rms)	230V
Slot depth, d_s	8 mm	Phase current (rms)	50
Tooth width, w_t	14 mm	Number of phase, m	3
Slot width, w_s	12 mm	Power factor, pf	0.79
Axial length of second rotor yoke, Y_{r2}	2.6 mm	Rated relative speed, $N_{r1} + N_{r2}$	12010 rpm
Number of series coil per phase, N_{ph}	19	Iron	M 22
Number of conductor per slote, N_{cs}	6	B_{sat}	1.7 T
		Width of bar, w_b	111mm
		Axial thikness of ring, l_r	8mm

VERIFICATIONS

The obtained design should be verified to see whether each point of machine core is under saturation or not. The flux lines and magnitude flux densities in the generator yokes can be computed and observed using a finite-element analysis software package. The obtained simulations for flux lines and flux magnitude densities at no-load and full-load conditions are shown in Fig. 12.

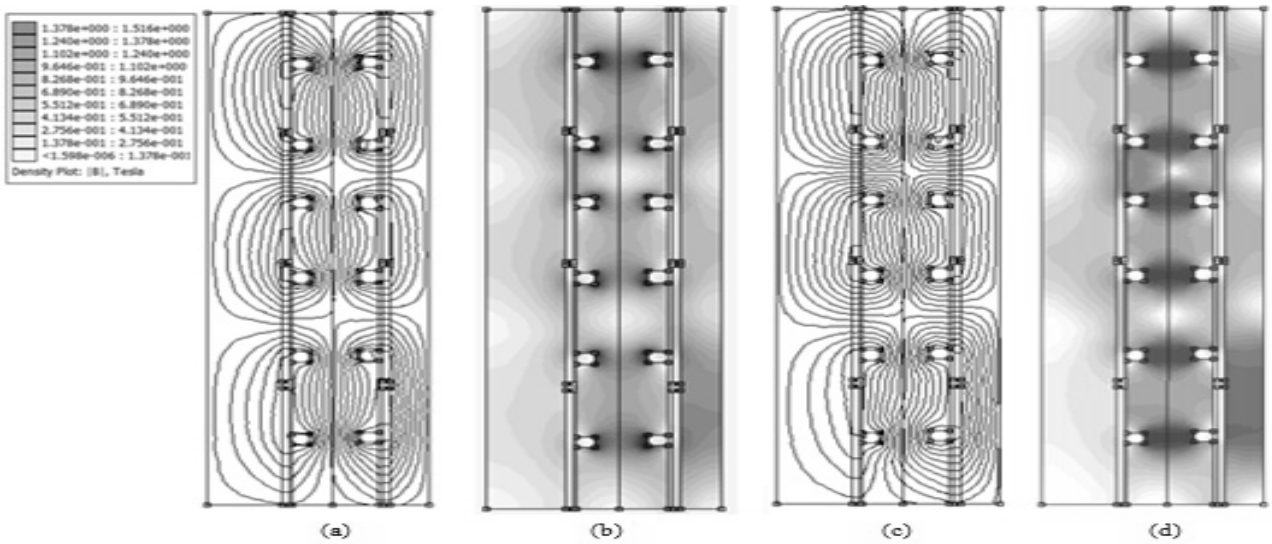

Figure 12. (a)Flux lines in full-load condition.(b) Flux densitty magnitude in no-load condition.(c) Flux lines in full-load condition.(d) Flux magnitude density in full load condition.

By reading through the values of flux magnetic densities in the generator cores points, it can be observed that the highest value of flux density is 1.6T while the saturation of the used iron happens at 1.8T.

CONCLUSION

This paper present the construction and design procedure of a novel type of permanent magnet generator with two mechanical power inputs. The design started with selection of initial data to reach primary design guarantee all cores are under saturation. It continued to reach a optimum light weight design by iteration of machine parameters. To observe the flux line and flux magnitude density in the obtained design a finite element analysis software package. The simulation results confirmed the effectiveness of the obtained design as well as the proposed topology.

REFERENCES

[1] Ocean Rnenewable Power Company. Acessed: Oct 2011. [Online]. Available: http://www.oceanrenewablepower.com/projects_florida.aspx, Feb. 12, 2012

[2] Marine Current Turbine. Acessed: Oct 2011. [Online]. Available: http://www.marineturbines.com/21/technology/aspx

[3] "A contra-rotating marine turbine on a flexible mooring: Development of a scaled prototype", 2nd International *Conference on Ocean Energy, ICOE* 2008, Brest, France. October 2008

[4] Clarke J A, Connor G, Grant A D and Johnstone C M. "Design and inintal testing of a contra-rotating tidal current turbine" Proc 6th European Wave and Tidal Energy Coference (2005), Glasgow

[5] hah, L. Cruden, A. Williams, B.W, "A Variable Speed Magnetic Gear Box Using Contra-Rotating Input Shafts," Magnetics, IEEE Trans, vol.42, no.2, pp.431-438, Feb, 2012

[6] Ferreira, et al., "Prototype of an Axial Flux Permanent Magnet Genarator for Wind Energy Systems Applications," in 12th *European Conference on Power Electronics and Applications*, EPE 2007, Aalborg, mark, 2007

[7] T. Sebastian, "Temperature effects on torqe prodcution and effeicecny of PM motors using NdFeB magents," IEEE Trans. Ind. Applicant., vol.31, pp. 353-357, Mar.Apr. 1990.

[8] A. Parviainen, "Design of axial-flux permanent-magnet low-speed machines and performance comparison be-tween radial-flux and axial-flux machines," *thesis of doc-torate*, Lappeeranta University of Technology, Lappeer-anta, Finland, 2005.

[9] Nima Amjady, Asghar Sfari-Doust, Abbas Rezaey, "A Novel Axial Flux Brushless Induction Generator with two Mechanical Power Inputs for Wind Energy Generation Applications" Journal of Basic and Applied Scientific Research (JBASR), vol.2, no.5 pp. 4812-4819,

[10] V.karami, m.J.Ketabdari, A.K.Akhtari "Paper numerical modeling of oscillating water column wave energy convertor," International Journal of Advanced Renewable Energy Research, Vol. 1, Issue.4, pp. 13-24, 2012

[11] Sumaira Tasnim, Amanullah Maung Than Oo, and Fakhrul Islam "Wind Generated Electricity: A Review of Generation,Transmission and Power Loss," International Journal of Advanced Renewable Energy Research, Vol. 1, Issue.4, pp. 25-45, 2012